Chapter

Sustainable and Efficient Hydroforming of Aerospace Composite Structures

Bo C. Jin, Xiaochen Li, Karl Neidert and Michael Ellis

Abstract

Hydroforming, in comparison with sheet stamping, is an efficient and economical manufacturing process for complex-shape aerospace composite parts because it does not require the use of a female die. The hydroforming manufacturing method is expected to greatly increase the formability of composite parts by using a controllable heated and pressurized fluid that acts as a support for the composite sheet throughout the forming process. The design of a hydroforming process and a machine to shape complex aerospace composite parts is proposed in this chapter. The design and analysis of a sheet metal hydroforming machine with composite overwrap are presented to sustainably and efficiently produce not only the aerospace composites but also dual-phase and bake hardened steel parts with complex 3D geometry.

Keywords: aerospace composite structures, sustainable manufacturing, hydroforming

1. Introduction

1.1 Background

Sheet hydroforming is a process that was primarily developed for the needs of the aircraft and aerospace industry. In sheet hydroforming, formed tooling blocks are placed in the loading tray of a pressure vessel, and pre-cut sheet metal blanks are placed over the blocks. Throw pads are then placed over the blanks to cushion sharp edges. The tray is then fed into the pressing chamber as a thick elastic blanket is unrolled over the tool and sheet metal. It is then backfill pressurized with hydraulic fluid under ultra-high pressure. The elastic fluid cell blanket diaphragm expands and flows downward over and around the metal blank. The sheet metal is pressed to follow the contour of the die block, exerting an even, positive pressure at all contact points. As a result, the metal blank is literally wrapped to the exact shape of the die block. The press is then depressurized for unloading the tray [1]. This process is ideal for prototyping and low volume production in aluminum, titanium, stainless steel, and other malleable aerospace alloys such as metal-composite panels in low volumes.

The primary pressure containment vessels used in these machines are designed to contain ultra-high pressures. In some cases, the internal pressures can be as high as 137.90 MPa (20,000 psi). In small diameter tubing this is a notable pressure.

However, as the diameter and area of the pressure chamber increases, the total pressure is applied to a significantly larger surface area, resulting in total loading forces that are exceedingly high.

Current designs in operation feature a traditional circular cross-section, a familiar geometry to most designers. However, the actual pressures exerted inside the chamber are not cylindrically uniform, as they would be in a fluid or gas pressure tank. Instead, the pressure loading originates from hydraulic working fluid inside a fundamentally rectangular shaped tray. These loads are then transferred into solid metal blocks called yoke plates that in turn each press against the walls of the pressure containment chamber with varying degrees of force.

The non-uniform pressure loading of the cylindrical pressure vessel wall results in localized forces that cause engineers to use excessive or unnecessary material, which increases both the weight and cost of the equipment **Figure 1**.

The objective of this project was to optimize the cross-sectional profile, attributes, and material usage of a pressure containment vessel for use in a hydroforming manufacturing press. The new design was to be preferable in cost, weight and overall performance. Finite element analysis was used extensively to validate the current operational design, material alternatives and the optimized cross-section designs proposed. The design is a modular construction consisting of several pressure containment sleeve rings fabricated from layers of radially axial wound high strength composite fiber filament infused with resin stabilizer over a metal liner. Into this envelope of several joined compression rings slides a movable pressure vessel that features a top-load clamshell cartridge type design. Integral to the lid of the forming chamber is a series of elastomeric tubes that work in unison to produce a type of a high-pressure hydroforming diaphragm. This modular "sleeve over sandwich" pressure containment scheme is designed to enable the system to be easily configured in various shapes, sizes and lengths. It is also conceived to improve functionality, capability and serviceability. Because of the unique properties of the design, it can be easily configured in various lengths so that a wide range of products can be produced including 100 kW wind turbine blades.

The proposed concept sets forth numerous innovative breakthroughs that infuse legacy hydroforming technology with renewed vigor and greatly improved competence. The design is conceived to deliver enhanced functionality, capability, cost and serviceability as well as resale value. State-of-the-art sensing and computation enable many of the advancements. The parametric geometrical modeling of the liner and composite overwrap was performed using FEA software [2] which is proved to be an

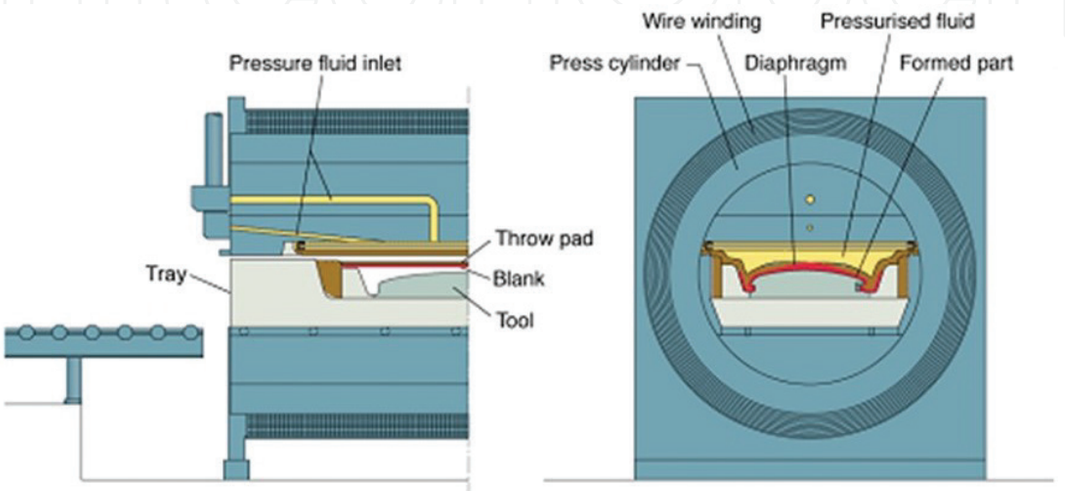

Figure 1.
Typical configuration of current commercial solutions (courtesy of Avure Inc.).

efficient method to verify the design and optimize geometry of advanced composite structures [3–10]. Parameters such as composite overwrap winding thickness, and the geometric outline of the liner and containment, were parametrically investigated to obtain optimized stress–strain relationships under hyper-pressure.

1.2 Objectives and structure

Currently the most powerful hydroforming pressure forming chambers are cylindrical constructions of high-strength, pre-tensioned steel wire wound over solid steel winding armatures. They are designed to meet "leak-rather-than-break" criteria". Some frames of this type can contain forces up to 137.89 MPa (20,000 psi) of operational pressure.

The objective of this project regarding the pressure containment system is to develop a non-cylindrical master section design that is comprised fundamentally of three elements: (a) Composite windings, b) a winding core, c() aluminum yoke plates. The design failure target for pressure containment is 165.47 MPa (24,000 psi). That is 137.89 MPa (20,000 psi) with a 20% safety factor or 110.32 MPa (16,000 psi) with a 50% safety factor. The containment section is intended to be configured to reduce weight significantly over "HS Steel Over Steel" chamber construction. It is intended to allow a completed machine to rest directly on a standard factory floor without additional floor structure reinforcements. The assumption for the proposed cylinder construction is composite over aluminum yoke plates. Composites may include glass, Kevlar 49, and carbon fibers. This study uses a carbon fiber source (Zoltek Panex 35 Continuous Tow pre-preg). The machine is meant to operate under cold shell start up conditions to 50% polymer plastic point. And the chamber operating temperature is assumed to be −17.78°C (0°F) to 48.89°C (120°F).

Aluminum alloys considered are 6061-T6 and 7075-T6. Windings and press frame are assumed for this study to be of matched metal type. Compressive strength of concrete for resting footprint loading is set at 17.24 MPa (2500 psi). The mechanism of operation of the machine assumes that pressure is applied by the injection of working fluid into a forming chamber cassette that has been loaded into the void area. The internal forming chamber cassette is not included in this modeling study. Pressure will be applied at full pressure to the side and horizontal walls of the inner yoke plate areas. The chamber has a fundamentally uniform cross section that is suited to sectional analysis. Loads will propagate from the inner void, into the yoke plates, into the winding frame and ultimately into the composite winding bobbin. Maximum vertical deflection at full pressure load of 165.47 MPa (24,000 psi) is assumed to be 6 mm.

If possible, it is desired that the design be low profile in appearance, resembling that of a toroidal ellipse section. This is desired to allow the installation and use of the machine without the addition of false load floors to support ergonomic reach over heights on larger than 1524 mm (60 in) wide forming cartridges. It is also assumed that a cosmetic outer cover may be applied to the cylinder design. This cosmetic cover will not be included in this design exploration. The project will begin with a baseline developed from a replication of a purely cylindrical design: "A". The effects of the loading properties will be applied to additional non-cylindrical designs B–E. The purpose of these designs is to build conceptual understanding by exploring radically unique cross-section designs. Based on these findings, special consideration is to be given to develop additional sections that may produce a design of reduced weight and cross-sectional height vs. a purely cylindrical design. The effects of steel vs. aluminum yoke plates are also to be investigated to compare strength to weight to size performance.

In Section 2 of this paper, we introduce the optimal design procedure and the design configurations A–E, and E1–E4. Sections 3 and 4 describe the results and discussion, and future perspective and opportunities.

2. Optimal design procedure

2.1 Basic structural configuration and FEA design parameters

Any composite overwrapped pressure vessel (COPV) design requires an analysis of the liner, the fiber overwrap, and the interaction between the two. COPV liners may be of ductile materials with only minimal load-sharing capabilities, such as ductile metal composites [11–19], glass fiber reinforced angle interlock composites [20–22], or carbon fiber reinforced composite oriented strand boards [5, 23–29].

The general layout and components of the baseline cross-section design (Section "A") are presented in **Figure 2a**. The outer diameter of Section "A" is roughly 60 cm. The design variables for the optimization of the circular cross-section "A" are presented in **Figure 2b**. These design variables are modified systematically throughout the design exploration procedure, allowing for different evolving design configurations.

In the same manner, four different probe locations were defined (**Figure 2c**) to obtain stress and displacement results of the tested cross-section designs and allow a quantitative comparison of the effects of each individual design variable, their respective interactions and the overall behavior of the different design configurations. These probing locations will be used for all the analysis carried out in order to obtain consistent results.

2.2 Yoke plate cutting angle concept

A new design concept referred to as "Yoke plate cutting angle" is introduced as a design variable. This unique concept provides control over the stress distribution at the yoke plates interface by means of a resulting friction force generated at the surface-to-surface contact interface. The angled (non-horizontal) contact interface between the yoke plates and side yoke plates allows both plates to work in unison to carry the pressure load while still providing some accommodation for stress deflection by allowing slip plane movement between the plates. The yoke plates' cutting

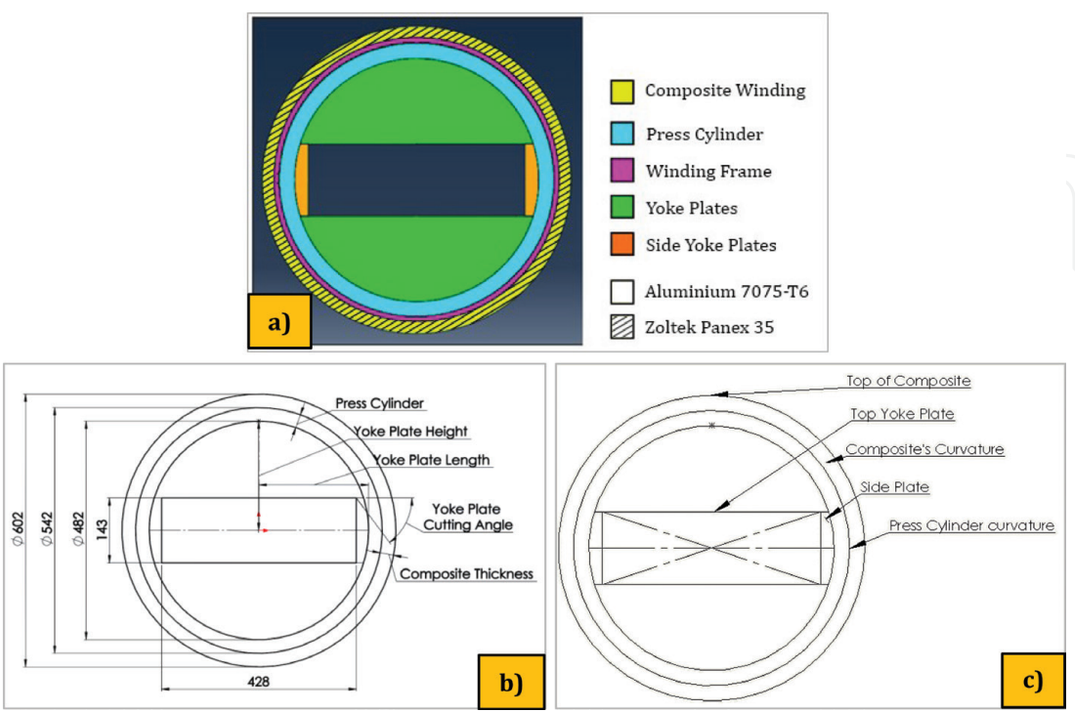

Figure 2.
(a) General component layout and materials used, (b) general dimensions and design parameters and (c) stress-probing locations.

Elastic modulus	E	71.7 GPa
Poisson	Nu	.33
Density	Rho	2.81e−9
Yield point	σ	503 MPa

Table 1.
Material properties of winding frame and yoke plates. (7075-T6 aluminum).

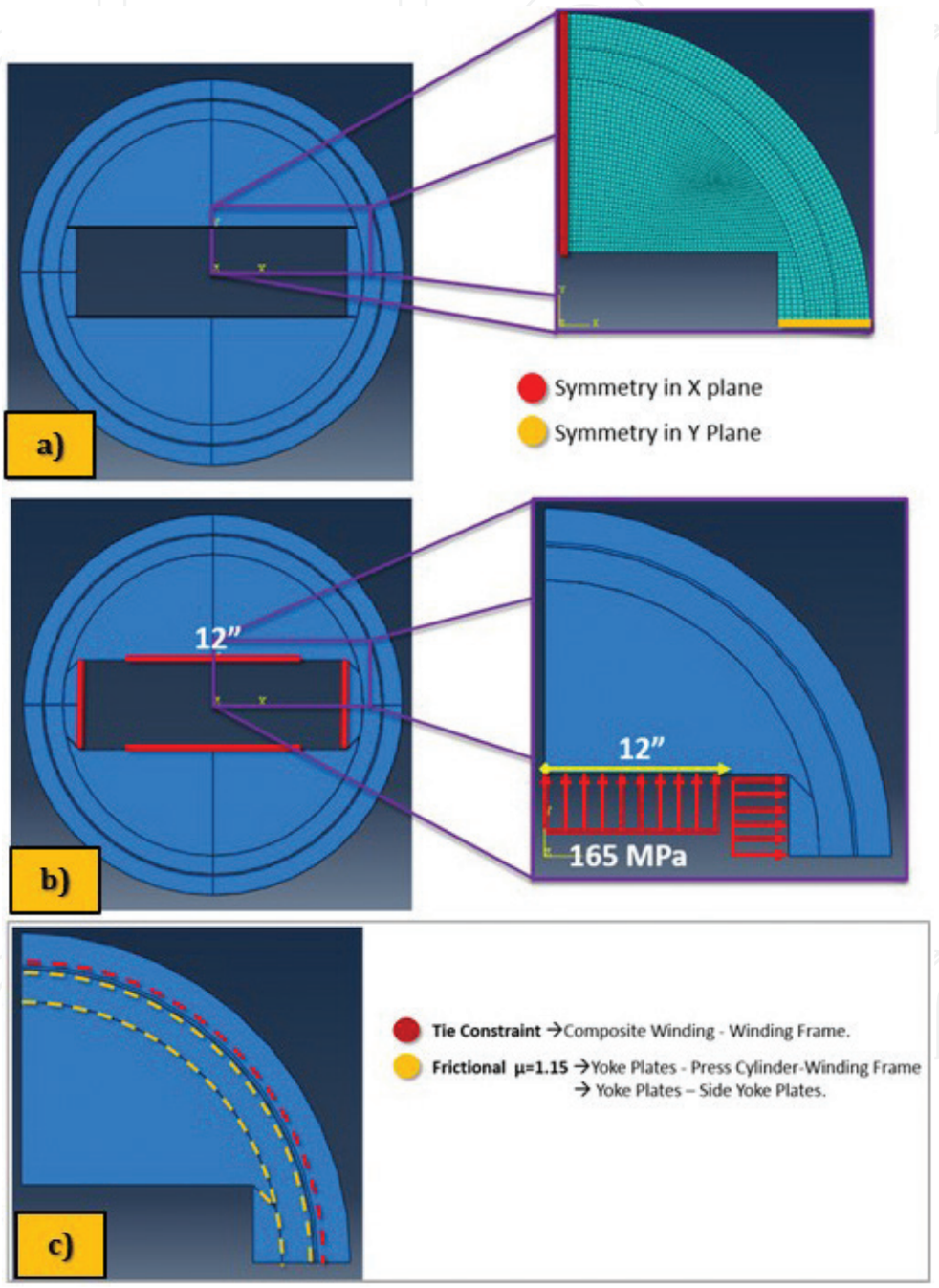

Figure 3.
(a) Boundary conditions and mesh, (b) applied loads and (c) contact definitions.

angle dictates the magnitude of the frictional force occurring at the interface. Thus, special attention must be paid to this dimension. A precise yoke plate cutting angle definition will allow contact related stresses to be just below the material's yield, while helping reduce the stress of the composite winding. Coulomb dry friction is a good starting point to approximate the maximum cutting angle that generates

a "stick" condition (no sliding) between the two surfaces. However, if no sliding occurs, stress concentration around the contact interface is bound to rise past the allowable limit—thus, some sliding must be ensured to provide stress relief.

2.3 General finite element model setup

2.3.1 Geometry and discretization

All the cross sections to be analyzed are expected to be symmetric in both horizontal and vertical directions due to the homogenous pressure that they are subjected to. The finite element models constructed, take full advantage of this geometric symmetry by simulating only one quarter of each cross section. This reduces computational time significantly **Table 1**.

Solid 3D elements with an approximate global size of 2.5 mm were used to create a fine mesh representative of the geometric features (**Figure 3a**).

2.3.2 Materials

The following material properties were applied to the aluminum yoke plates and winding frame:

For the composite winding, carbon fiber prepreg (Zoltek Panex 35) was used. This material's properties are presented in **Table 2**.

2.3.3 Boundary conditions

Symmetry boundary conditions were applied as shown in **Table 3**.

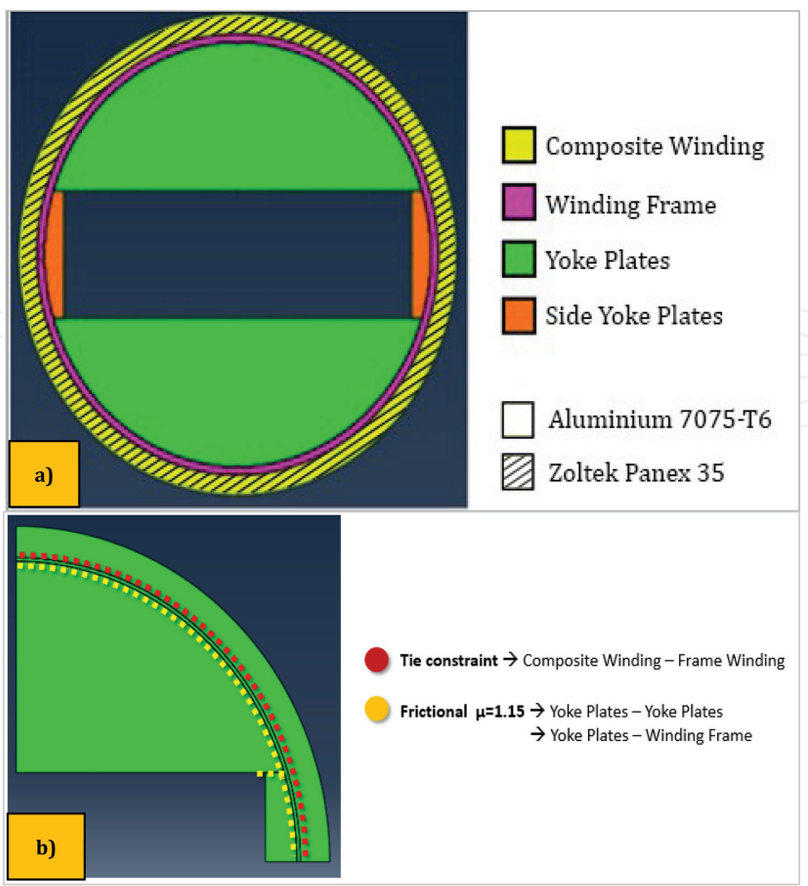

Figure 4.
(a) Updated cross-section assembly without press cylinder tube and (b) updated contact definition.

2.3.4 Loading conditions

A homogenous pressure of 165 MPa is applied to the inner faces of the yoke plates as shown in **Figure 3b**.

2.3.5 Contact definition

Frictional contacts were defined between the yoke plates and the winding frame (**Figure 3c**). A tie constraint was used to bond the winding frame and the composite winding, as it is assumed that no movement occurs between these two components.

2.3.6 Section "A" test matrix

Section "A" is a pure circular cross section imitative of that of commercially available hydroforming machines with similar operating pressure capabilities. However, these dimensions must be optimized for the use of composite winding instead of the traditional pre-tensioned steel wire.

The test matrix for the Section "A" optimization is presented in **Table 4**. The non-horizontal angled cut contact interface between yoke plates is introduced as an additional design variable with the intention of reducing yoke plates stress, while the press cylinder thickness is reduced until it is completely removed.

2.3.7 Updated finite element model without press cylinder

Following the results obtained from the analysis of section "A," the finite element model assembly was modified. The new assembly is essentially the same as the original, with the exception that the press cylinder has been removed, and the yoke plates were extended to fill out the space of the press cylinder. The same materials are used for each component. Likewise, the same symmetry conditions and load cases are applied.

Elastic modulus 1	E1	134 GPa
Elastic modulus 2 & 3	E2, E3	129 GPa
Poisson ratio	Nu12, Nu13, Nu23	0.34
Shear modulus	G	4.84 GPa
Density	Rho	2.81e−9
Failure stress	σ	1903 MPa

Table 2.
Composite winding material properties (Zoltek Panex 35 carbon Prepreg [30]).

Symmetry plane	**Degrees of freedom**					
	Translation			**Rotation**		
	Tx	**Ty**	**Tz**	**Rx**	**Ry**	**Rz**
X	0	Free	Free	Free	0	0
Y	Free	0	Free	0	Free	0

Table 3.
Symmetry boundary conditions.

ID #	Composite thickness	Press cylinder thickness	Yoke plate radius	Plate cutting angle
1	30	30	241	0
2	30	30	241	−45
3	30	40	241	0
4	30	30	241	45
5	30	30	241	90
6	30	30	251	45
7	30	30	251	−45
8	30	10	261	−45
9	25	0	261	−45, rounded corners
10	25	0	251	−45, rounded corners
11	25	0	241	−35, rounded corners
12	25	0	241	0
13	25	0	241	0, rounded corner

Table 4.
Section "A" design configurations test matrix.

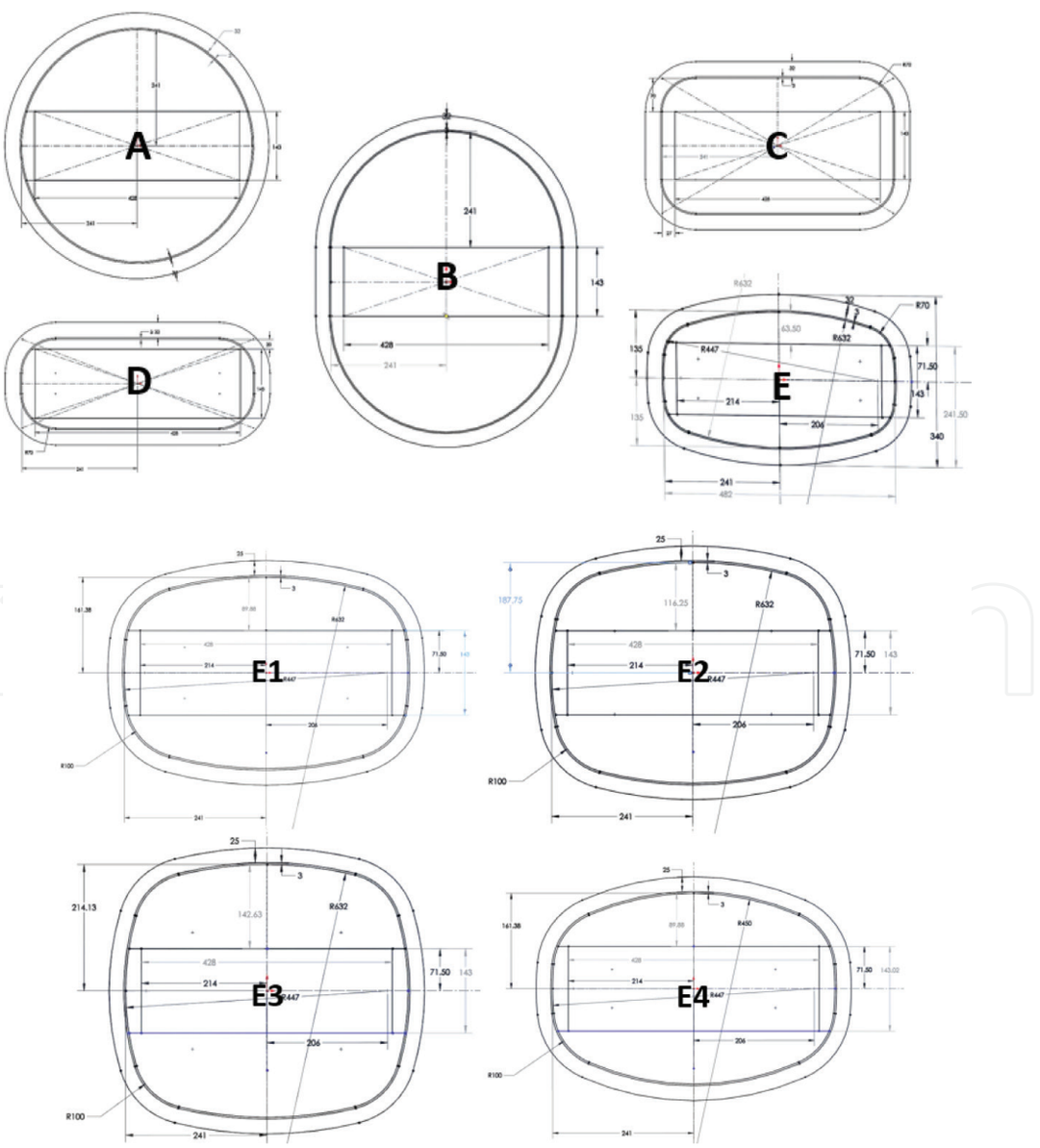

Figure 5.
Proposed cross section shapes A, B, C, D, E and E variants.

2.3.8 Updated contact definition

Without the press cylinder component, the yoke plates are in direct contact with the winding frame, so a new frictional contact was added between these two parts, shown in **Figure 4b**.

2.4 Finite element models for sections "B," "C," "D," and "E"

A similar finite element model and analysis was carried out for the rest of the cross-section designs shown in **Figure 5**. This design aims to determine the effect of the reduced overall cross section height, and different curvatures applied to the main shape of the cross section. However, due to the removal of the press cylinder, the subsequent models were readjusted as previously shown in 2.3.7 & 2.3.8.

2.5 Variations of section "E"

In an effort to improve the performance of the promising section "E", additional designs derived from section "E" were analyzed (**Figure 5**). Moreover, a design matrix (**Table 5**) was constructed based on defined design parameters: composite

		25mm Composite Winding						35mm Composite Winding								
		Aluminium			Steel			Aluminium			Steel					
		Corner Radius			Corner Radius			Corner Radius			Corner Radius			Max. Stress (MPa.)		Displacement
Design #	Section	0 mm.	10 mm.	20 mm.	0 mm.	10 mm.	20 mm.	0 mm.	10 mm.	20 mm.	0 mm.	10 mm.	20 mm.	Composite	Yoke Plate	Yoke Plate
25	E1	1	0	0	0	0	0	0	0	0	0	0	0	2038.0	4534.0	11.3
26	E1	0	1	0	0	0	0	0	0	0	0	0	0	2004.0	4377.0	11.7
27	E1	0	0	1	0	0	0	0	0	0	0	0	0	1949.0	3375.0	12.0
28	E1	0	0	0	1	0	0	0	0	0	0	0	0	1269.0	6701.0	6.6
29	E1	0	0	0	0	1	0	0	0	0	0	0	0	1234.0	6516.0	6.8
30	E1	0	0	0	0	0	1	0	0	0	0	0	0	1178.0	4938.0	6.8
31	E1	0	0	0	0	0	0	1	0	0	0	0	0	1668.0	3982.0	9.4
32	E1	0	0	0	0	0	0	0	1	0	0	0	0	1648.0	3864.0	9.7
33	E1	0	0	0	0	0	0	0	0	1	0	0	0	1620.0	2979.0	10.0
34	E1	0	0	0	0	0	0	0	0	0	1	0	0	1102.0	6078.0	5.8
35	E1	0	0	0	0	0	0	0	0	0	0	1	0	1079.0	5930.0	5.9
36	E1	0	0	0	0	0	0	0	0	0	0	0	1	1038.0	4515.0	6.0
37	E2	1	0	0	0	0	0	0	0	0	0	0	0	1393.0	3642.0	6.3
38	E2	0	1	0	0	0	0	0	0	0	0	0	0	1390.0	3666.0	6.4
39	E2	0	0	1	0	0	0	0	0	0	0	0	0	1372.0	2866.0	6.4
40	E2	0	0	0	1	0	0	0	0	0	0	0	0	815.9	5269.0	3.3
41	E2	0	0	0	0	1	0	0	0	0	0	0	0	805.7	5206.0	3.3
42	E2	0	0	0	0	0	1	0	0	0	0	0	0	792.0	3981.0	3.3
43	E2	0	0	0	0	0	0	1	0	0	0	0	0	1155.0	3182.0	5.5
44	E2	0	0	0	0	0	0	0	1	0	0	0	0	1151.0	3225.0	5.5
45	E2	0	0	0	0	0	0	0	0	1	0	0	0	1134.0	2534.0	5.5
46	E2	0	0	0	0	0	0	0	0	0	1	0	0	707.2	4833.0	3.0
47	E2	0	0	0	0	0	0	0	0	0	0	1	0	697.4	4818.0	3.0
48	E2	0	0	0	0	0	0	0	0	0	0	0	1	684.4	3703.0	3.0
49	E3	1	0	0	0	0	0	0	0	0	0	0	0	1009.0	3096.0	4.2
50	E3	0	1	0	0	0	0	0	0	0	0	0	0	1005.0	3309.0	4.2
51	E3	0	0	1	0	0	0	0	0	0	0	0	0	997.9	2279.0	4.3
52	E3	0	0	0	1	0	0	0	0	0	0	0	0	542.6	4488.0	2.1
53	E3	0	0	0	0	1	0	0	0	0	0	0	0	538.7	4709.0	2.1
54	E3	0	0	0	0	0	1	0	0	0	0	0	0	534.3	3196.0	2.1
55	E3	0	0	0	0	0	0	1	0	0	0	0	0	849.8	2710.0	3.7
56	E3	0	0	0	0	0	0	0	1	0	0	0	0	845.3	2923.0	3.7
57	E3	0	0	0	0	0	0	0	0	1	0	0	0	838.2	2021.0	3.7
58	E3	0	0	0	0	0	0	0	0	0	1	0	0	484.2	4132.0	1.9
59	E3	0	0	0	0	0	0	0	0	0	0	1	0	479.4	4374.0	1.9
60	E3	0	0	0	0	0	0	0	0	0	0	0	1	473.8	2979.0	1.9
61	E4	1	0	0	0	0	0	0	0	0	0	0	0	2033.0	5196.0	11.9
62	E4	0	1	0	0	0	0	0	0	0	0	0	0	2019.0	4792.0	12.4
63	E4	0	0	1	0	0	0	0	0	0	0	0	0	1970.0	3705.0	12.8
64	E4	0	0	0	1	0	0	0	0	0	0	0	0	1347.0	8145.0	7.2
65	E4	0	0	0	0	1	0	0	0	0	0	0	0	1308.0	7519.0	7.4
66	E4	0	0	0	0	0	1	0	0	0	0	0	0	1242.0	5687.0	7.5
67	E4	0	0	0	0	0	0	1	0	0	0	0	0	1659.0	4515.0	9.9
68	E4	0	0	0	0	0	0	0	1	0	0	0	0	1642.0	4173.0	10.2
69	E4	0	0	0	0	0	0	0	0	1	0	0	0	1613.0	3223.0	10.6
70	E4	0	0	0	0	0	0	0	0	0	1	0	0	1153.0	7285.0	6.3
71	E4	0	0	0	0	0	0	0	0	0	0	1	0	1120.0	6741.0	6.4
72	E4	0	0	0	0	0	0	0	0	0	0	0	1	1075.0	5125.0	6.5

*Red cells are above the material's Yield/Strength Point

Table 5.
Section E variations test matrix.

	Design variables					Results (MPa)				
ID	Composite thickness	Plate height	Plate length	L/H ratio	Plate cutting angle	Composite stress at top	Composite stress at curvature	Top plate stress	Side plate stress	Displacement (mm)
13	25	241	241	1	0	665	1807	355	383	2.98
14	25	200	250	1.25	0	1052	2002	587	432	5.21
15	25	200	250	1.25	0	1098	1983	628	538	4.93
16	25	200	300	1.5	0	1434	2173	852	457	8.38
17	25	200	300	1.5	−35	1395	2018	843	777	8.38
18	25	220	242	1.1	45	1428	2268	990	423	9.2
19	25	220	242	1.1	0	791	1762	440	515	3.16
20	30	220	242	1.1	−35	779	1690	519	459	3.36
21	27.5	210	231	1.1	−25	848	1895	467	386	3.25
22	27.5	200	231	1.155	−30	933	1711	533	357	3.71
23	25	206	228	1.1122	−35	910	1863	501.15	750	3.5
24	25	200	228	1.14	−35	979	1991	541	366	3.84
25	25	205	230	1.122	N/A	926	1846	513	445	3.51
26	25	200	225	1.125	N/A	942	1898	518	397	3.4
27	25	201	222	1.1045	N/A	930	2098	503	496	3.22
28	27.5	201	222	1.1045	N/A	876	1796	488	477	3

Table 6.
Design optimization test matrix.

thickness, yoke plate material and corner radius. This allowed for a systematic testing procedure to evaluate the performance of the different configurations product of the multiple design parameter combinations.

2.6 Section "A": ellipsoidal optimization

Section "A" was found to offer superior structural properties compared to the other designs analyzed in this project. This section allows for the smoothest stress distribution along the composite winding. However, as previously stated, the design exploration aims to find a cross section with a smaller height, such as section "E" (**Figure 5**). Given the poor performance of the custom designed sections (B–E, E1–E4) a new design exploration was carried out by defining the main geometry as an ellipse. By varying the major and minor axis dimensions, subsequently, a more systematic approach was adopted for the optimization of the cross section. Section "A" was used as the starting point, and from there, the design variables (**Figure 2b**) were parameterized. The test matrix for the ellipsoidal optimization of the cross section is presented in **Table 6**. Configuration 13 is the previously optimized circular section and is used as the baseline for this optimization. The objective is to reduce the overall height and material usage.

3. Results

3.1 Section "A" optimization results

As part of the optimization process intended to reduce the overall height and material usage of the pressure vessel's cross section, the press cylinder was removed from the design. A noticeable lack of stress near the yoke plates interface (**Figure 6a**) encouraged the addition of an angled cut (non-horizontal) interfaces between the yoke plates. The advantages of using a non-horizontal yoke plate contact interface are visible in the results for design configurations 2, 8, 9 (**Figure 6b, 9c**, & **9d**, respectively), as the stress near the contact of the yoke plates increases substantially but remains below the material yield point. A decrease in the press cylinder stress was also achieved, so the press cylinder thickness was gradually reduced (**Figur 6c**) until it was completely removed from the assembly. With the press cylinder removed, we concluded that the angled yoke plates' interfaces were not essential, since a simpler horizontal allowed for stress magnitudes within the required limits, as depicted in **Figure 6e** (configuration 13). This resulting cross section design obtained from the optimization process was set as the base for the subsequent optimization procedures, and the finite element model was modified to account for the removal of the press cylinder, as described in 2.3.7 & 2.3.8.

3.2 Section "B," "C," "D," and "E" FEA results

Sections "B," "C," "D," and "E" showed a considerably inferior performance to section "A." However, the surface area of their yoke plates and their overall height (with the clear exception of Section "B") was considerably less than that of section "A." The substandard performance of these sections can be directly associated with the change in curvature of the composite winding due to the change in the height-to-length ratio for the overall cross section. As this ratio increases (height < length), the curvature radius decreases, and thus, stress concentrations appear in the

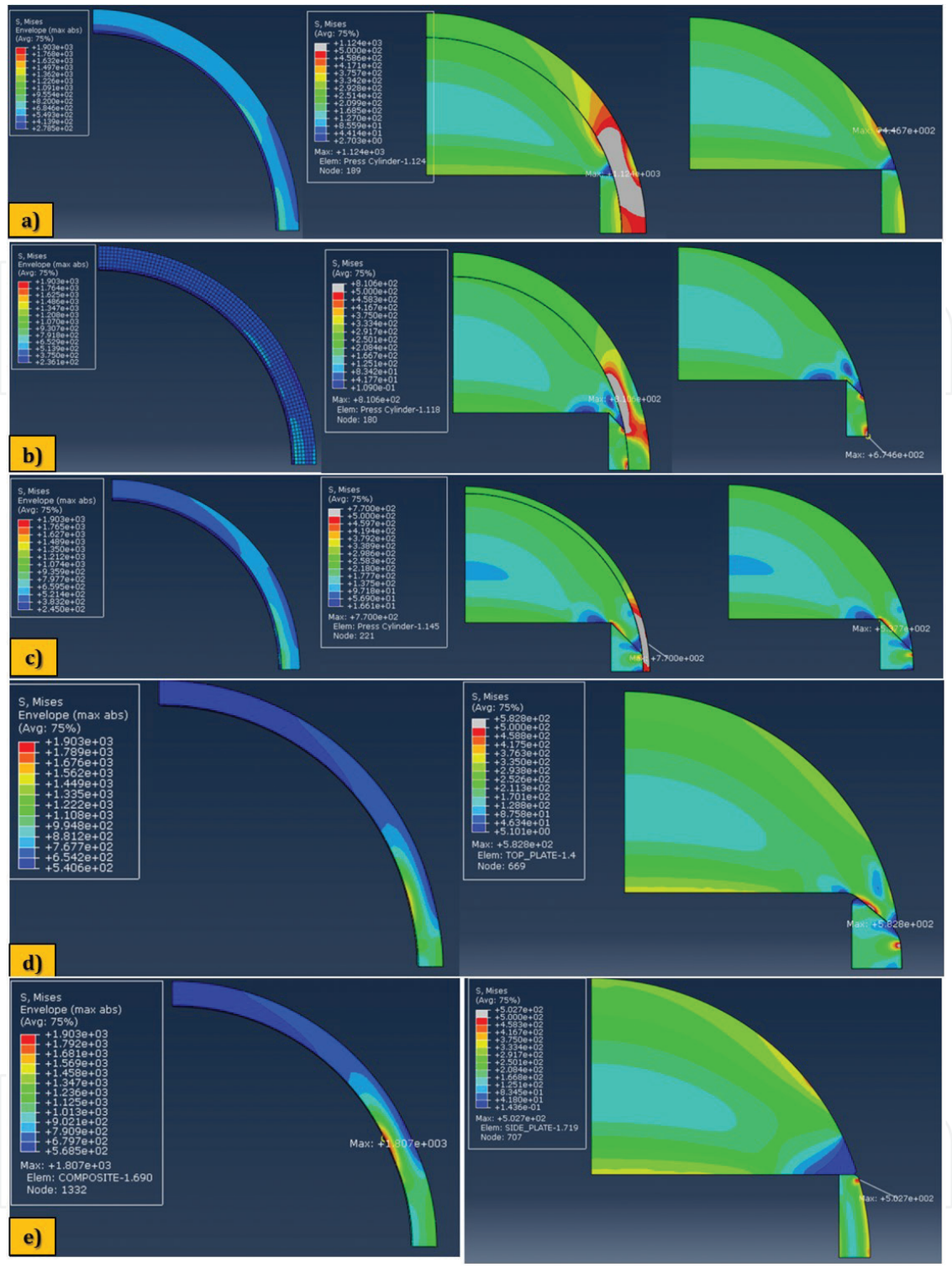

Figure 6.
Stress results for ellipsoidal section design configurations: (a) configuration 1, (b) configuration 2, (c) configuration 8, (d) configuration 9, (e) configuration 13.

composite winding. However, a small length-to-height ratio (height > > length) similar to Section "B" is also undesired, as the stress in the side plates increases considerably.

As is the case with section "A" results, a noticeable lack of stress near the yoke plates interface is observed in the results for sections "B," "C," and "D". Likewise, the stress magnitude on the side yoke plates is less than that of the main yoke plates. A non-horizontal angled cut contact interface could have been implemented for

these sections, however, the stress on the composite winding is well above its limit in all sections, and thus, the angled contact interface would've been of little use for these configurations as they were proposed. The results for these sections are presented in **Figure 7**.

3.3 Section "E" variants FEA results

The section E variants appeared to be the ideal candidates for an optimized designed. This was not the case, as the E section proved not to be strong enough to withstand the applied pressure load. The failure mechanism was primarily located in the composite winding, at the inner surface of the corner rounds. To reduce the stress at this location, the corner radii must be increased, although to achieve this, the height of the yoke plates must be increased, which represents a step back

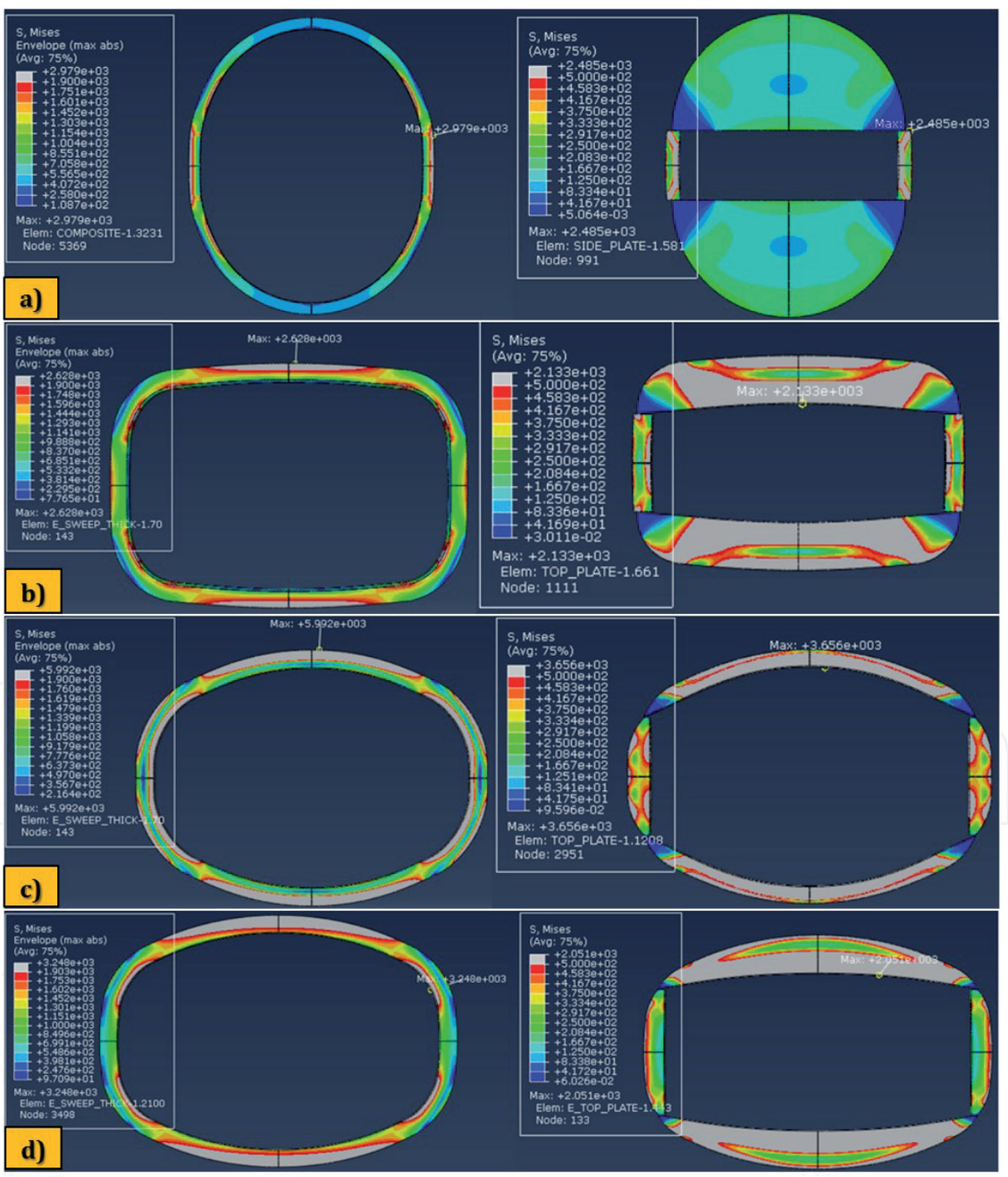

Figure 7.
Stress results for: (a) section "B," (b) section "C," (c) section "D," (d) section "E".

toward the original circular cross section design. We concluded that cross sections that tightly wrap around the inner slot where the pressure is applied are most likely to stress beyond the permissible limit, primarily due to high stress concentration around the sharp radii near the corners. Due to the failure of all the design configurations proposed in the test matrix for Section "E" variations (**Table 5**), only the stress results for the baseline configurations for each custom Section E1–E4 are provided in **Figure 8** to illustrate the stress concentration areas in the different cross section designs.

As stated before, none of the custom design sections (B–E & E1–E4) resulted in feasible designs. Returning to the last feasible configuration (Section "A," design configuration 13), a new design exploration was carried out by defining the main geometry as an ellipse. By varying the major and minor axis dimensions, an ellipsoidal shape with a smaller height was achieved. The design intent and evolution are shown in **Figure 9**, where stress results for key design iteration are provided. The minor axis is reduced considerably during the first configurations, increasing the length-to-height ratio and consequently the stress responses. The minor axis had to be increased back again until the design stress limits were met. Different non-horizontal angled cut contact interfaces were also tested, such as, 45° and −35° interface angles. Based on results and the original idea behind the concept, we concluded that the non-horizontal contact interface must have a negative angle (on the right side of the vertical symmetry plane) with respect to the horizontal plane to be beneficial for the design (achieve load transfer from yoke plate to side yoke plate). The stress results demonstrate that the length-to-height ratio is an important design parameter, which must be close to 1 to achieve good stress distributions along the composite winding. Regardless of the final configuration length-to-height ratio being close to one, i.e., the cross section being almost circular, a considerable reduction in cross section height was achieved.

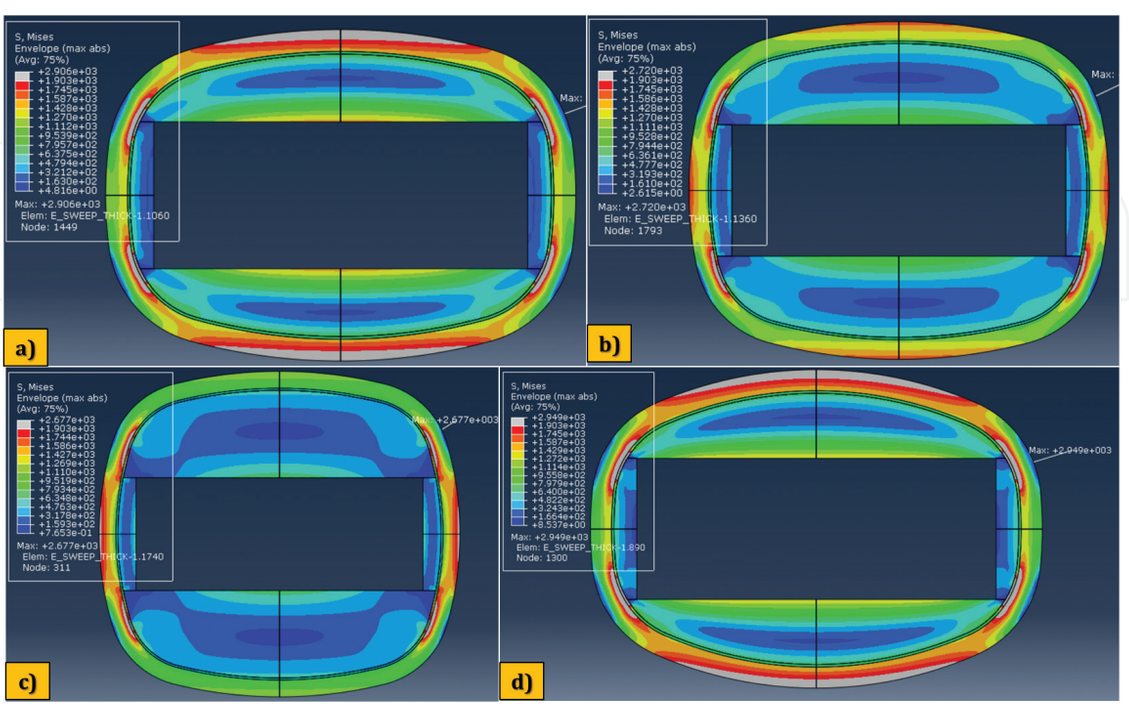

Figure 8.
Stress results for section "E" variations design configurations: (a) section E1, (b) section E2, (c) section E3, (d) section E4.

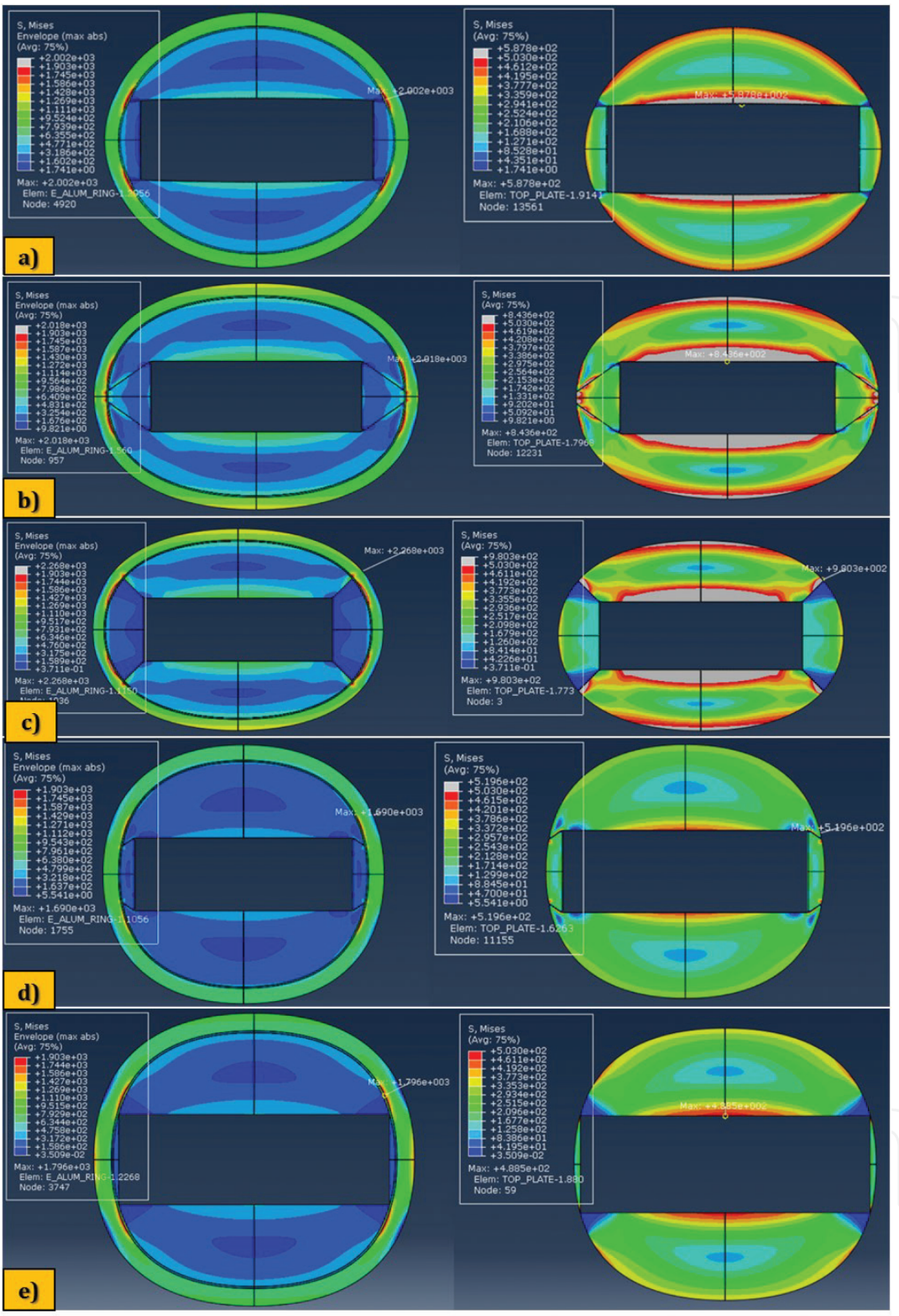

Figure 9.
Stress results for the design configurations produced during the ellipsoidal optimization procedures. (a) Configuration 15, (b) configuration 17, (c) configuration 18, (d) configuration 20, (e) configuration 28.

3.4 Ellipsoidal optimization of circular section "A" FEA results

3.5 Optimization results

A feasible design configuration (**Figure 10**) resulted from this design exploration (marked green in **Table 5**). At first view, it appears to be nearly circular,

although it is not. The section has a length-to-height ratio of 1.1045 while maintaining stress concentrations within the allowable limit. The optimized curvatures resulting from the specially selected design parameters provide a reduction of up to 23% (139 mm) on the total cross section height when compared to the original Section "A" design (including press cylinder) (602 mm), or 14% when compared to the optimized circular section "A" without the press cylinder. Similarly, the overall height of the yoke plates was reduced 25% with respect to the original section "A." One particular drawback of the proposed design is the necessary increase in composite winding thickness. A more detailed sensitivity analysis can help determine the optimal composite winding thickness between the bounds set forward by this work in order to adjust the maximum stress on both the composite winding and yoke plates to be equal to the predefined design stress (yield stress).

Note that the yoke plate surface area subjected to pressure is twice as large as that of the side yoke plates. Thus, a greater net force is exerted on the top and bottom yoke plates when compared to the side plates. The applied pressure load produces outward displacement or expansion of the whole structure. However, the composite winding tends to expand more in the vertical direction due to the greater surface area producing a higher total magnitude of force. The vertical displacement generates a contraction of the sides of the composite structure, which opposes the expansive behavior caused by the lateral pressure load. Consequently, the resultant lateral forces acting upon the sides yoke plates have a considerably smaller magnitude than that of the vertical force. This allows for the use of very side yoke plates, as shown in configuration 28. A non-horizontal angled cut is not practical for these design configurations due to the reduced width of the side yoke plates. Otherwise, it may well be possible to further reduce yoke plate height by means of a non-horizontal yoke plate contact interface.

Note that the increase in composite winding thickness may induce additional manufacturing costs, which must be studied in detail. The overall advantage of having a reduced cross section height must be of significant value to justify the increase in cost due to additional composite material. A through manufacturing analysis would be beneficial to determine whether the cost of increasing the composite material usage or increasing the overall yoke plate size yields the best possible outcome.

3.6 ANOVA: analysis of variance of design variables

Finite element analysis results of each parameterized configuration proposed in the test matrix for Section "E" variations were statistically tested to estimate the

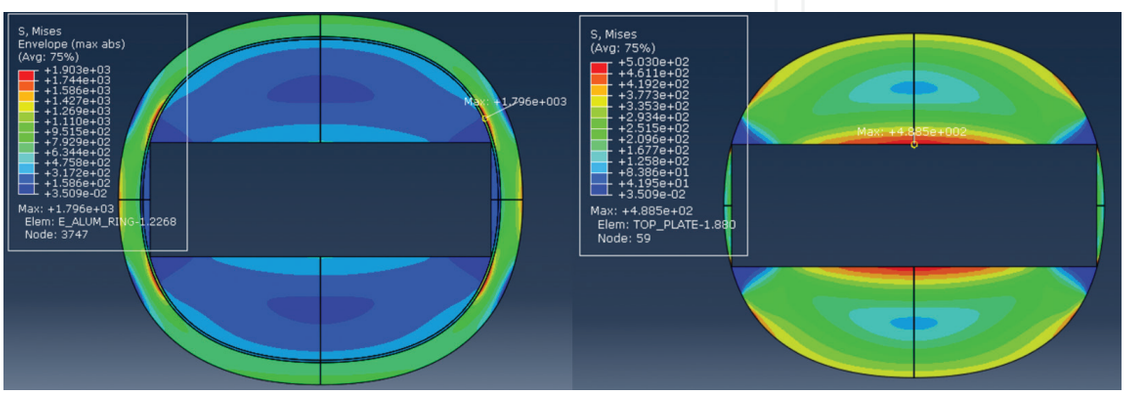

Figure 10.
Ellipsoidal optimization design configuration 28 stress results.

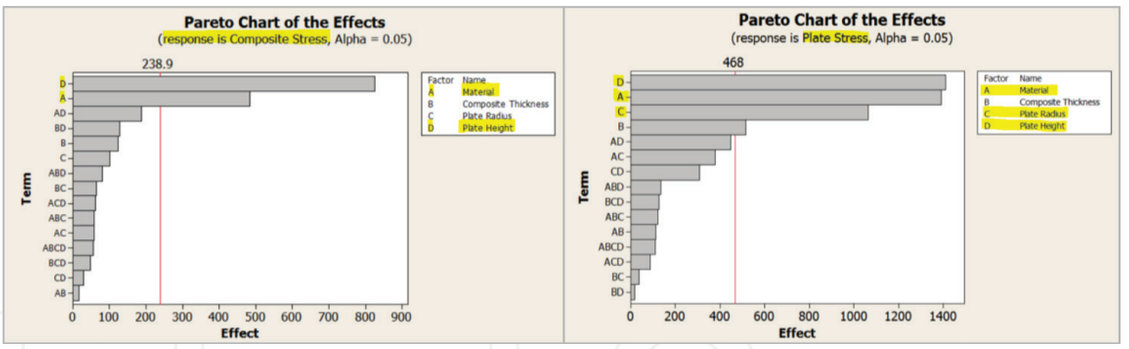

Figure 11.
Effect of design parameter on composite winding stress and yoke plate stress respectively.

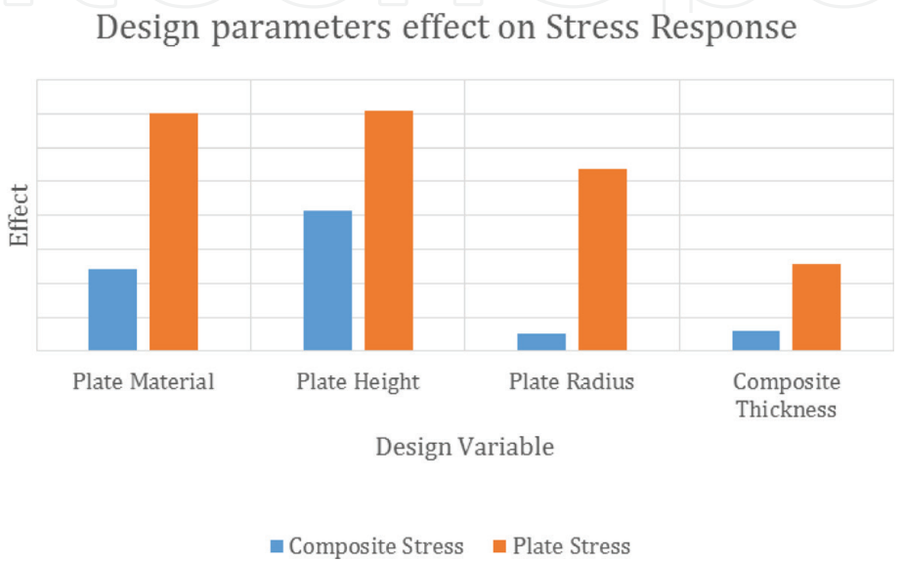

Figure 12.
Accumulative effect of design parameter on composite winding stress and yoke plate stress.

effect of each design variable and their possible combined effects on the maximum stress. An analysis of variance (ANOVA) of the stress response at a specific point in the geometry of each design configuration exposes which design parameter has the greatest effect on the composite winding and yoke plate stresses of the model, respectively (shown in the form of Pareto charts in **Figure 11**). In most cases, plate height has the greatest effect on both stress and displacement responses, followed by the yoke plates material. Aluminum yoke plates show better performance than their steel counterparts.

The accumulated effects in **Figure 11** are plotted in **Figure 12** to illustrate the principal and most sensitive response. It can be concluded that Yoke plate stress is the most sensitive response to changes in the design parameters for custom sections E1–E4.

4. Conclusions

In this study, a multi-physics approach was employed to derive the performance of a type of pressure vessel. Pressure loads were transferred asymmetrically through multiple materials and geometries. The mechanical properties and FEA of various section types were investigated.

The results of the study demonstrate that pressure containment of 165.48 MPa (24,000 psi) is feasible using carbon fiber bobbin wound over a 7075-T6 yoke plate. The simulations show that asymmetric internal loading of a rectangular high-pressure zone containing working fluid does indeed create localized hot spots of pressure in both the containment windings and the associated yoke plates. The primary surprise is that bridge-like bending deflection in the yoke plates is one of the major concerns of the system. This bending deflection caused catastrophic containment winding failure to occur at the centerline of the outer containment windings. Yoke plate deformation would also ultimately cause forming chamber deflection and leakage.

The study reinforces the idea that a near-circular cross section provides the best overall stress distribution throughout the composite winding. However, this comes at the expense of increasing the overall size of the yoke plates. By modifying the design parameters, principally the yoke plates' height, and adjusting the composite winding to seamlessly wrap around the new configuration, a reduction in the yoke plate size is achieved while attaining stress concentrations below each material limit.

L/H ratio defines the overall curvature of the composite, and the closer it gets to 1, the better the performance. However, the stress in the composite is most of the time less than its strength. The main problem has to do with the yoke plates. Early study sections 20–23 have round cross sections, but the stresses induced into the yoke plates exceed the yoke plate's material yield point, thus must be discarded.

Analysis of variance (ANOVA) of the stress responses at a specific point in the geometry reveal that yoke plate section height, yoke plate material, and the overall cross-section curvature radius (length-to-height ratio) are the driving design parameters to achieve a successful and improved solution.

One of the key findings of relevance is the use of an angled wedge integral to the upper yoke plate to create a positive pressure transfer shear plane with the side yoke plates. This positive surface-to-surface contact area allows for lateral expansion compression pressure loads be transferred into the upper yoke plate as surface tension. This additional tension induced into the upper plate helps to stabilize the "bridge bending" tendency of the upper and lower yoke plates. It also reduces the loads transferred by the side yoke plates into the outer fiber windings by confining lateral yoke plate movement expansion.

After testing greatly varied profiles and cross sections, we conclude that a near-round ellipse section successfully accommodates a pressure of 165.48 MPa (24,000 psi). This is using mildly interfacing yoke plates to balance the structure. This solution is conceptually similar to a traditional legacy design section configuration. However, this conclusion is a point of reference - not a final design. It should be considered a proof-of-concept validation point that illustrates that a cross section can be developed to meet the functional performance criteria required using carbon fiber and aluminum in place of steel. As a result, the section as it stands offers a significant reduction in weight over the traditional "steel over steel" fabrication method. A thin-wall section, light weight, reduction or elimination of press cylinder wall achieves a 65% overall weight reduction in similar design due to a shift from steel wound with high tensile steel tape to aluminum wound with carbon fiber.

5. Future perspectives

The pressure containment vessel cross section design can be further optimized by using more organic curve geometry instead of the more traditional arc or ellipse curvatures to define it. Smooth and progressive curve curvatures are expected to allow more gentle and controlled application of pressure load forces.

An improved lower profile design may be possible with additional design revisions. It is believed that a design that has a near vertical yoke plate outer side wall surface to surface interface that also uses the interlocking yoke slip plate design concept developed may produce a better overall performance.

The final functional design will also need to accommodate various voids for fluid ingress and egress as well as valves, electronics and assembly. The use of surface typology optimization will allow the extraction of as much unnecessary sectional mass as possible. This will be helpful in establishing the correct location of these voids.

Author details

Bo C. Jin[1*], Xiaochen Li[1], Karl Neidert[2] and Michael Ellis[3]

1 Aerospace and Mechanical Engineering, University of Southern California, United States

2 Karl Neidert and Associates, United States

3 Ellis Industrial Design, San Diego, CA, United States

*Address all correspondence to: bochengj@usc.edu

References

[1] Emprotech Corp. Emprotech Corp. [Online]. Available from: http://www.enprotech.com/

[2] SIMULIA Dassault Systems. ABAQUS Theory Manual. Providence; 2012

[3] Jin B, Pelegri A. Three-dimensional numerical simulation of random fiber composites with high aspect ratio and high volume fraction. Journal of Engineering Materials and Technology. 2011;**133**:41014

[4] Wu H, Xu W, Shan D, Jin B. An extended GRN model for low stress triaxiality and application in spinning forming. Journal of Materials Processing Technology. 2019;**263**:112-128

[5] Jain A, Jin B, Nutt S. Mean field homogenization methods for strand composites. Journal of Composites Part B. 2017;**124**:31-39

[6] Jin B, Li X, Jain A, Wu M, Mier R, Herraez M, et al. Prediction of stiffness of reused , carbon fiber/epoxy composite oriented strand board using finite element methods. Recycling materials & structures. Feature article. Society for the Advancement of Material and Process Engineering (SAMPE) Journal. 2017;**53**:32-39

[7] Jin B, Li X, Jain A, Herraez M, Gonzalez C, LLorca J, et al. Development of a finite element model for reused carbon fiber epoxy composite oriented strand board. In: Proceedings of SAMPE 2016; Long Beach. 2016

[8] Jin B, Li X, Mier R, Pun A, Joshi S, Nutt S. Parametric modeling, higher order FEA and experimental investigation of hat-stiffened composite panels. Journal of Composite Structures. 2015;**128**:207-220

[9] Jin B, Joshi S, Pun A, Nutt S. Design sensitivity of hat-stiffened composite panels. In: Proceedings of American Society for Composites Conference 2014; San Diego. 2014

[10] Jin B, Liu W, Patel H, Nutt S. Application of MSC NASTRAN UDS in modeling and analysis of a hybrid composite reinforced conductor core. In: Proceedings of MSC NASTRAN Conference 2013; Los Angeles. 2013

[11] McLaughlan PB, Forth SC. Composite Overwrapped Pressure Vessels, A Primer. Houston; 2011

[12] Ma H, Xu W, Jin B, Shan D, Nutt S. Damage evaluation in tube spinnability test with ductile fracture criteria. International Journal of Mechanical Sciences. 2015;**100**:99-111

[13] Wu H, Fan G, Jin B, Geng L, Cui X, Huang M. Fabrication and mechanical properties of TiBw/Ti-Ti (Al) laminated composites. Journal of Materials and Design. 2016;**89**:697-702

[14] Wu H, Fan G, Jin B, Geng L, Cui X, Huang M, et al. Enhanced fracture toughness of TiBw/Ti3Al composites with a layered reinforcement distribution. Journal of Materials Science and Engineering: A. 2016;**670**:233-239

[15] Wu H, Jin B, Geng L, Fan G, Cui X, Huang M, et al. Ductile-phase toughening in TiBw/Ti-Ti3Al metallic-intermetallic laminate composites. Journal of Metallurgical and Materials Transactions A. 2015;**46**:3803-3807

[16] Chen Z, Huang T, Jin B, Hu J, Lu H, Nutt S. High yield synthesis of single-layer graphene microsheets with dimensional control. Journal of Carbon. 2014;**68**:167-174

[17] Huang T, Li T, Xin Y, Jin B, Chen Z, Su C, et al. Preparation and utility of a self-lubricating and anti-wear graphene oxide nano-polytetrafluoroethylene hybrid. Journal of RSC Advances. 2014;**4**:19814

[18] Huang T, Jin B, Li X, Li T, Nutt S. Experimental and finite element analysis study of load carrying capacity of modified polyimide. In: Proceedings of SAMPE 2013; Wichita. 2013

[19] NASA. A Theoretical Investigation of Composite Overwrapped Pressure Vessel (COPV) Mechanics Applied to NASA Full Scale Tests. Houston; 2009

[20] Jin L, Jin B, Kar N, Nutt S, Sun B, Gu B. Tension-tension fatigue behavior of layer-to-layer 3D angle-interlock woven composites. Journal of Materials Chemistry and Physics. 2013;**140**:183-190

[21] Jin L, Niu Z, Jin B, Sun B, Gu B. Comparisons of static bending and fatigue damage between 3D angle-interlock and 3D orthogonal woven composites. Journal of Reinforced Plastics and Composites. 2012;**31**(14):935-945

[22] Ma Q, Wang K, Wang S, Liu H, Jin B, Jin L, Ma P. Tensile damage mechanism of 3-D angle-interlock woven composite using acoustic emission events monitoring. Autex Research Journal. 2018;**18**(1):46-50

[23] Jin B, Li X, Jain A, Carlos G, LLorca J, Nutt S. Optimization of microstructure and mechanical properties of composite oriented strand board from reused prepreg. Journal of Composite Structures. 2017;**174**:389-398

[24] Wu M, Jin B, Nutt S. Processing and performance of recyclable composites for wind turbine blades. Advanced Manufacturing: Polymer & Composites Science. 2019;**12**:12-28

[25] Jin B, Li X, Jain A, Wu M, Mier R, Herraez M, et al. Mechanical properties and finite element analysis of reused UD carbon fiber/epoxy OoA VBO composite oriented strand board. In: Proceedings of SAMPE 2016; Long Beach. 2016

[26] Jin B, Li X, Wu M, Jain A, Jormescu A, Gonzalez C, et al. Nondestructive testing and evaluation of conventional and reused carbon fiber epoxy composites using ultrasonic and stitched micro-CT. In: Proceedings of SAMPE 2016; Long Beach. 2016

[27] Jain A, Jin B, Li X, Nutt S. Stiffness predictions of random chip composites by combining finite element calculations with inclusion based models. In: Proceedings of SAMPE 2016; Long Beach. 2016

[28] Jain A, Jin B, Nutt S. Development of chip composites with improved mechanical performance attributes using hybrid multi-scale modelling methods. In: Proceedings of CAMX 2016; Anaheim. 2016

[29] Jin B. Recent development of reused carbon fiber reinforced composite oriented strand boards. Chapter 8 of Book: Recent Developments in the Field of Carbon Fibers. IntechOpen. DOI: 10.5772/intechopen.71346

[30] Zoltek. PANEX 35 commercial carbon Fiber. In: Material Specs Sheet.